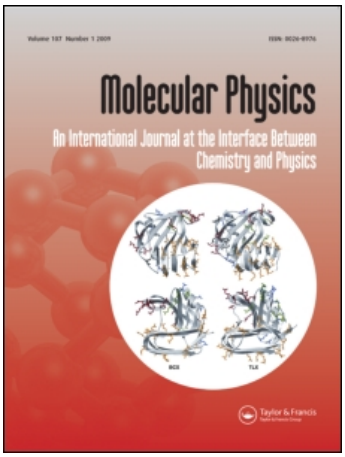

Molecular Physics
Publication details, including instructions for authors and subscription information:
http://www.informaworld.com/smpp/title~content=t713395160

The far infrared absorption spectrum of liquid nitrogen

Jannis Samios [a]; Uwe Mittag [a]; Thomas Dorfmüller [a]
[a] Fakultät für Chemie, Universität Bielefeld, Bielefeld, F.R. Germany

Online Publication Date: 20 October 1985

To cite this Article Samios, Jannis, Mittag, Uwe and Dorfmüller, Thomas(1985)'The far infrared absorption spectrum of liquid nitrogen',Molecular Physics,56:3,541 — 556
To link to this Article: DOI: 10.1080/00268978500102511
URL: http://dx.doi.org/10.1080/00268978500102511

MOLECULAR PHYSICS, 1985, VOL. 56, NO. 3, 541–556

The far infrared absorption spectrum of liquid nitrogen
A molecular dynamics simulation study

by JANNIS SAMIOS, UWE MITTAG and THOMAS DORFMÜLLER†
Fakultät für Chemie, Universität Bielefeld,
D-4800 Bielefeld, F.R. Germany

(*Received 15 February 1985; accepted 2 June 1985*)

The interaction quadrupole-induced dipole correlation function and the corresponding absorption spectrum of liquid nitrogen have been simulated in a site-site molecular dynamics calculation at atmospheric pressure and 66 K. Two models were used: an anisotropic and an isotropic molecular polarizability model. The differences between the two models are significant, but small. The results were compared to the published absorption spectra and reasonable agreement was obtained. The differences between simulation and experiment are discussed in terms of the properties of the model used. The total dipole correlation function was analysed in terms of a self-term and a cross-term. The contribution of the latter, which is negative, is quite large. Furthermore, a number of correlation functions describing the details of the molecular motion in the liquid have been calculated and are discussed in view of a possible discrimination between rotational/translational motions and/or single-molecule/collective motions.

1. INTRODUCTION

The dynamics of molecular systems at liquid densities present serious problems which cannot easily be discussed in terms of an extrapolation of the properties of less dense systems. This is mainly due to the many-body character of the pertinent interactions and the small distances between interacting molecules. Both features, i.e. the inadequacy of the pair potential approach and our incomplete knowledge of the intermolecular potential at small distances, can only be bypassed by quite restrictive and often not well-assessed assumptions. Under these conditions we only obtain a partial description of the phenomena and at present the best we can expect from our efforts is an assessment of and possibly an increase in the range of validity of the system of underlying assumptions. The shape of spectral lines represents a useful experimental access to the molecular dynamics of liquids. However, the complete description of the latter by spectral measurements would, at least in principle, involve the use of spectral moments extending to higher orders (actually to infinite order). Since this is not feasible for practical reasons, we can make an attempt to illuminate the problem by using different kinds of correlation functions (CFs) which stress different aspects of the problem.

† Author to whom all correspondence should be addressed.

In view of this situation, molecular dynamics simulations have proved an invaluable tool in performing 'experiments' under controlled conditions with idealized particles. We are thus in a position to calculate quantities which are experimentally accessible in real liquids and other quantities which, although not directly observable, may prove useful in obtaining an insight into the details of molecular dynamics of liquids.

Our objective in this study is to calculate a number of time CFs which pertain to some of the details of the molecular motion in liquid nitrogen and especially to those which underly the shapes of the interaction—induced far infrared absorption spectra. In particular, we present some results on liquid nitrogen at 66 K and atmospheric pressure and compare them to the available experimental data.

The absorption spectrum of nitrogen has been thoroughly studied in the gas phase by a number of authors [1–3]. On the contrary, the spectral studies of liquid nitrogen are much less numerous. One study reports the absorption spectrum at 76 K [4] and two other studies give somewhat more extensive data at 66 K [3] and at 90 K [5] respectively. The interpretation of the gas phase spectra is quite straightforward, since the spectrum can be well approximated by the envelope of the unbroadened rotational lines produced by transitions between the quantum levels of the rotational motion of quadrupole-induced dipoles. On the other hand, the situation is much less clear in the liquid phase. Firstly, the intensity is much lower than one would expect by extrapolation of the gas data to liquid densities. Secondly, the shape of the spectra is wider with more intensity in the high-frequency range than this is the case for the gas under similar conditions. Both effects can be qualitatively understood in terms of the local cancellation of the field anisotropy [6] and by the increased importance of short-range higher multipole induction effects in the dense phase respectively [7]. However, this interpretation of the liquid phase spectra is incomplete, as it neglects many-particle interactions and their time dependence. The theory is still restricted to the formulation of the time dependence of pairwise-additive interactions between proximate molecules. Another source of incertitude is our ignorance of the extent of translation–rotation coupling in many liquid systems.

The dynamics of liquid nitrogen has been dealt with to some extent by Steele and Birnbaum [8], who calculated the two lower-order moments of the far infrared absorption spectrum in view of obtaining the contribution of the three-body correlations. On the other hand Guillot and Birnbaum [9], working with a quadrupole induction mechanism and a predominantly isotropic intermolecular potential, have calculated the far infrared spectrum of liquid nitrogen as a convolution of a translational and a rotational spectrum. Their theoretical spectrum obtained by this method reproduces to a certain extent the experimental spectrum, however it seems to lack some of the high frequency components of the former.

The simulation of the properties of liquid nitrogen has been based upon a site-site potential [10], which has given quite reliable results for the static and dynamic properties. A simulation of the far infrared absorption spectrum [3] on the basis of quadrupole–induced dipoles and an isotropic polarizability of liquid nitrogen near the triple point has produced a spectrum with a shape very similar to the experimental spectrum. However, the maximum absorptivity of the simulated spectrum is smaller by a factor of 4 than the experimental result.

Under the usual assumptions made in this kind of simulation and the dominance of the quadrupole-induction mechanism, as well as the use of a particular

intermolecular potential, we felt that a study of the molecular dynamics of liquid nitrogen could be helpful in solving some of the discrepancies which are still poorly understood. We therefore chose to calculate several of the various CFs describing the single molecule motion, the collective motion of the environment of a reference molecule, the so-called 'cage', and the possible cross corelations between different components of the complex motions occurring in the liquid. We shall use the term 'cage' for the ensemble of molecules which surround the reference molecule restricting its motion and which are the source of the dipole-inducing electrical field. In the simulation this cage is precisely defined by the cut-off radius, in the experiment it is based upon the range of the interactions. Note that this term does not imply a rigid and/or a permanent structure.

The total induced dipole CF, $C_{\mathbf{M}}(t)$, which is a convenient representation of the time dependence of the experimental far infrared spectra, is defined by the following equation:

$$C_{\mathbf{M}}(t) = \langle \mathbf{M}(0) \cdot \mathbf{M}(t) \rangle, \tag{1}$$

where the total induced moment of a sample of N molecules is

$$\mathbf{M}(t) = \sum_{i=1} \boldsymbol{\mu}_i(t), \tag{2}$$

$$\boldsymbol{\mu}_i(t) = \sum_{j \neq i} \boldsymbol{\mu}_{ij}(t). \tag{3}$$

The moment induced by the molecule j on a reference molecule i, the distance between the two being $\mathbf{R}_{ij}(t)$, is $\boldsymbol{\mu}_{ij}(t)$. The absorption coefficient due to the time dependence of the ensemble of the induced intermolecular dipoles in the sample is linked to the induced dipole CF defined in (1) by equation (4) [11].

$$\alpha(\omega) = \frac{2[n^2 + 2]^2 \omega \tanh\left(\dfrac{\hbar\omega}{2K_B T}\right)}{27 n \varepsilon_0 V c \hbar} \int_0^\infty C_{\mathbf{M}}(t) \cos \omega t \, dt, \tag{4}$$

n is the refractive index of the liquid assumed frequency independent, V the volume of the sample, the other constants having their usual significance. The local field correction is given by the Onsager expression $n((n^2 + 2)/3n)^2$ [11].

To begin with, we have calculated the following quantities:

(*a*) $C_{\mathbf{M}}(t)$ both for an isotropic and an anisotropic molecular polarizability model respectively and the corresponding absorption spectra.

(*b*) The self- and the cross-CFs $C_s(t)$ and $C_+(t)$ defined as follows:

$$\langle \mathbf{M}(0)\mathbf{M}(t) \rangle = \sum_{i=1} \langle \boldsymbol{\mu}_i(0)\boldsymbol{\mu}_i(t) \rangle + \sum_{i \neq j} \langle \boldsymbol{\mu}_i(0)\boldsymbol{\mu}_j(t) + \boldsymbol{\mu}_j(0)\boldsymbol{\mu}_i(t) \rangle, \tag{5a}$$

$$C_{\mathbf{M}}(t) = C_s(t) + C_+(t). \tag{5b}$$

The self-term describes the time evolution, i.e. the loss of coherence, of the dipole moment induced on a given reference molecule by the cage molecules. The cross-term describes the time evolution of the magnitude and the relative position of the two induced dipole moments on all the molecular pairs i, j in the sample. Higher order correlations, i.e. i, j, k and i, j, k, l etc. are included in the self and cross-CFs respectively as defined in equation (5). They have been recently calculated separately by Steele [12]. The study of the time dependence of the two CFs

can contribute to the understanding of the details of the dynamics of this liquid as only their sum is directly accessible to the far infrared experiment. The analysis of the total CF into the two components is essential to describing the molecular motion in the liquid as reflected by the far infrared interaction induced spectrum. The theoretical spectra have been calculated by fitting the analytical Mori expression to the CFs and by calculating the analytical Fourier transform of the expression obtained.

2. The induction mechanism: induced dipole correlation functions and far infrared spectra

The two following assumptions have been generally used in the simulation of interaction-induced effect, namely the point multipole expansion [13] for calculating the local field and the point polarizability assumption to obtain the induced dipole moments on the molecules. Both assumptions are approximations to the situation where the intermolecular distances are large as compared to the molecular dimensions. The basically correct description of interaction-induced effects by a distributed electronic charge and hence by non-localized polarizability cannot be practically exploited for MD simulations, as the theoretical description of this model is still in its infancy. An example of a somewhat simpler description is the atom polarizability model of Applequist [14], which is not easily applicable to most molecular systems. Thus, it is not possible to describe the overall polarizability of CS_2 by two isotropic polarizability tensors located on the S-atoms of the molecule or at some other appropriate positions. On the other hand, such a description is feasible for the nitrogen molecule and for this reason we have attempted to assess the impact of both the anisotropic molecular polarizability and the atom polarizability models on the simulated molecular dynamics of liquid nitrogen. Here, we present the results for the first model, whereas the calculations pertaining to the second model, using the molecule configurations obtained in the present simulation, are underway. The one-point multipole expansion of the molecular inducing charges gives the potential ϕ_{ij} at the mass centre of the reference molecule i produced by the electric charge distribution of the molecule j located at a distance R_{ij} from the reference molecule

$$\phi_{ij}(R_{ij}) = \frac{Q}{R_{ij}} + \frac{\mu_\alpha R_{ij}^\alpha}{R_{ij}^3} + \frac{\Theta_{\alpha\beta}}{3R_{ij}^5}\left[3R_{ij}^\alpha R_{ij}^\beta - R_{ij}^2\delta_{\alpha\beta}\right] + \ldots. \tag{6}$$

The electric moments of increasing order are defined as follows:

$$Q = \sum_i e_i, \tag{7a}$$

$$\mu_\alpha = \sum_i e_i r_i^\alpha, \tag{7b}$$

$$\Theta_{\alpha\beta} = \sum_i e_i[3r_i^\alpha r_i^\beta - r_{ij}^2\delta_{\alpha\beta}]/2. \tag{7c}$$

The indices α, β, γ $(= X, Y, Z)$ represent the cartesian coordinates in a laboratory fixed system, e_i is the local charge and $\mathbf{r}_i$ its position vector.

The lowest order multipole of N_2 is the quadrupole, the next higher being a hexadecapole. Assuming provisionally that the former is the dominant, i.e.

neglecting the hexadecapole, we can calculate the local field and the corresponding induced dipole moments on the reference molecule by means of the equations

$$\mathbf{F}_{ij}(R_{ij}) = -\nabla\left[\frac{1}{3R_{ij}^5}(3R_{ij}^{\alpha}R_{ij}^{\beta} - R_{ij}^2\delta_{\alpha\beta})\right]{}^{j}\Theta_{\alpha\beta}, \tag{8a}$$

$$\boldsymbol{\mu}_{ij}(t) = \boldsymbol{\alpha}_i(t) \cdot \mathbf{F}_{ij}(t). \tag{8b}$$

This calculation can be carried out in a straightforward manner on the basis of the distances $R_{ij}(R_{ij}^{\alpha}, \alpha = x, y, z)$ and the quadrupole tensor ${}^{j}\Theta_{\alpha\beta} = 1/2\theta(3u_j^{\alpha}u_j^{\beta} - \delta_{\alpha\beta})$ furnished by the simulation of the liquid. θ is the molecular quadrupole, $\mathbf{u}_i(t)$ the unit vector at the time t located along the molecular axis of the reference molecule i in the laboratory reference system and $\boldsymbol{\alpha}_i$ the polarizability tensor of the molecule. However, whereas some authors have calculated the induced dipole moment $\boldsymbol{\mu}_{ij}$ by analysing the polarizability into the isotropic polarizability component Tr and the anisotropy $\alpha^{\parallel} - \alpha^{\perp}$ [6(c), 12, 15], we chose to calculate in the first instance the components of the inducing field $\mathbf{F}^{\parallel}$ parallel and $\mathbf{F}^{\perp}$ normal to the molecular axis and then multiplying these with the corresponding components $\alpha^{\parallel}$ and $\alpha^{\perp}$ of the polarizability tensor.

$$\begin{aligned}\boldsymbol{\mu}_{ij}(t) &= \alpha^{\parallel}[(\mathbf{F}_{ij}(t)\mathbf{u}_i(t))\mathbf{u}_i(t)] + \alpha^{\perp}[\mathbf{F}_{ij}(t) - \mathbf{F}_{ij}^{\parallel}(t)] \\ &= \boldsymbol{\mu}_{ij}^{\parallel} + \mu_{ij}^{\perp}(t).\end{aligned} \tag{9}$$

This procedure was used because it allowed us to calculate not only the total self-CF $C_s(t)$, but also the components of the self-CF $C_s^{\parallel}(t)$ and $C_s^{\perp}(t)$ parallel and normal to the molecular axis as well as the cross-CF $C_+(t)$ between the dipoles induced in different molecules according to equation (5) and the cross-CF $C_s(t)$ between the parallel and the normal components induced on a given reference molecule. This proved to be quite instructive in the case of the simulation of CS_2 [15] since all CFs reflect different aspects of the complex molecular mobility in the liquid. We expect a coordinated discussion of the shapes of these different CFs to give us an improved picture of the detailed dynamics in the simulated model liquid. It appears for example, as will be shown below, that the cross-CF $C_+(t)$ is far from being negligible, and consequently it is not legitimate to identify the CF of the molecular induced dipole to the total induced dipole. The importance of this cross-term is indeed obvious since it contains information about the loss of intermolecular coherence in the liquid.

In order to compare the simulation results with the available experimental data and to discuss the molecular dynamics on the basis of the pertinent CFs it is necessary to parallel the simulated and the experimental results of both, the time CFs and the spectra. The transformation from the former to the latter and vice-versa was carried out both by numerical Fourier transformation using equation (4) and, independently, by fitting the 3-variable equation given in equation (10) to the data and subsequently, using the analytical Fourier transform of this expression given in equation (12) below.

The fit function for the CFs used was

$$C_{\mathbf{M}}(t) = \frac{\Gamma}{1+\Gamma}\exp(-\alpha_2 t) + \frac{1}{1+\Gamma}\left[\frac{\alpha_1 + \Gamma\alpha_2}{\beta}\sin\beta t + \cos\beta t\right]\exp(-\alpha_1 t). \tag{10}$$

The parameters in these equations are defined as follows:

$$\Gamma = \frac{2\alpha_1[\alpha_1^2 + \beta^2]}{\alpha_2[-3\alpha_1^2 + \alpha_2^2 + \beta^2]}, \tag{11 a}$$

$$\alpha_1 = \tfrac{1}{2}[S_1 + S_2] + \frac{\gamma}{3}, \tag{11 b}$$

$$\alpha_2 = -[S_1 + S_2] + \frac{\gamma}{3}, \tag{11 c}$$

$$b = \frac{\sqrt{3}}{2}[S_1 - S_2], \tag{11 d}$$

$$S_1 = \left[-\frac{B}{2} + \left(\frac{A^3}{27} + \frac{B^2}{4}\right)^{1/2}\right]^{1/3}, \tag{11 e}$$

$$S_2 = \left[-\frac{B}{2} - \left(\frac{A^3}{27} + \frac{B^2}{4}\right)^{1/2}\right]^{1/3}, \tag{11 f}$$

$$A = K_0(0) + K_1(0) - \frac{\gamma^2}{3}, \tag{11 g}$$

$$B = \frac{\gamma}{3}\left[\frac{2\gamma^2}{9} + 2K_0(0) - K_1(0)\right]. \tag{11 h}$$

At this point it should be noted, that the expression for Γ given in some instances in the literature is incorrect [16]. The correct form given in (11 *a*) has been checked by inverse Laplace transformation of $C(i\omega)$ using the Heaviside theorem to produce $C_{\mathbf{M}}(t)$.

The Mori three-variable spectral function, given in equation (12) below, is derived, as indicated in (1), by a Fourier transform of $C_{\mathbf{M}}(t)$.

$$\alpha(\omega) = E\,\frac{\gamma K_0(0)K_1(0)\omega^2}{\gamma^2[K_0(0) - \omega^2]^2 + \omega^2[\omega^2 - (K_0(0) + K_1(0)]^2}. \tag{12}$$

The three constants γ, K_0 and K_1 in this equation are known functions of the constants appearing in (10) and defined in equations (11 *a–h*).

The amplitude of the spectrum is determined by the amplitude factor E in (12) which is proportional to the square of the effective dipole moment of the absorbing molecule. The effective dipole moment $\bar{\mu}_{\text{eff}}^2$ is a convenient and physically meaningful measure of the absorption and is calculated from the experimental absorption spectrum by means of equation (13) or from the unnormalized simulated total CF at zero time.

$$\bar{\mu}_{\text{eff}}^2 = \frac{54\varepsilon_0 K_\beta T}{\pi}\,\frac{M}{\rho N}\,\frac{nC}{(n^2+2)^2}\int_{\text{band}}\frac{\alpha(\tilde{\nu})}{\tilde{\nu}^2}\,d\tilde{\nu}, \tag{13}$$

N, M, c, ρ, ε_0 are the Avogadro number, the molecular mass, the light velocity, the density of the liquid and the vacuum refractive index respectively.

3. Technical details of the computation

The simulation was carried out on an ensemble of 256 rigid diatomic molecules in a cube with periodic boundary conditions. The potential was a Lennard-

Jones type site-site potential. We have used two different sets of potential parameters both of which have been used previously in the literature [10(a), (c)]. The distance between the two nitrogen atoms was taken equal to $d = 1{\cdot}1$ Å. The initial temperature was 66 K corresponding to a number density of $\rho = 0{\cdot}01864\,\text{Å}^{-3}$. This point of the phase diagram is located near the triple point. Two different algorithms were used, the Verlet-Singer algorithm [17] with a time step of $4{\cdot}4 \times 10^{-15}$ s and a quaternion predictor corrector algorithm [18] with a time step of 5×10^{-15} s. The computational details of this work are tabulated in table 1 together with the corresponding information from the two other simulations reported in the literature. The table shows that the three different simulations of liquid nitrogen differ in one or more of the characteristic features listed. A comparison of the results can, in principle, give us a clue as to the importance of quantities like the number of molecules in the box, the size of the time step, the value of the potential parameters and the total number of configurations calculated. The last mentioned feature of the simulation, i.e. the total number of the configurations calculated, is essential in determining the quality of the statistics obtained. For obvious reasons this number has been restricted in many calculations, a procedure which, together with the periodic boundary conditions [19], entails an incertitude in the CFs at longer times which cannot be easily assessed. It appears that, in the case of linear molecules like N_2, if the statistics are sampled only from times below 50 ps in real time, the accuracy of the shape of the total CF shown in figure 1 is not satisfactory particularly at time shifts above 0·35 ps. Thus, in order to come to a well founded result, we have extended the calculation to 90 ps. After this time the obtained CF was fairly stable.

Equilibrium was achieved after approximately 10 ps. The data were stored at intervals of 0·025 ps. The thermodynamic properties calculated from these configurations were identical with the ones reported in the two other simulations mentioned. Since the quaternion predictor-corrector algorithm produced smaller fluctuations in the thermodynamic properties than the Verlet–Singer algorithm the former was used predominantly. Our total CFs have been calculated with two different sets of potential parameters, as indicated in table 1. The differences between the results were, however, not important and therefore, in order to allow a better comparison, we present here only the data obtained from the parameter set which was also used in the studies [10(a)] and [3].

The calculation of the induced moments from the simulated configurations requires experimental values for the polarizability components and the quadrupole moment of the nitrogen molecule. These values were taken from the literature. Since the quadrupole values reported in the literature do not agree two different characteristic experimental values were used in order to delimitate the range of the validity of the calculated data [20]. The induced dipole on a given reference molecule i has been calculated for all pairs ij where j comprises all molecules $i \neq j$ fulfilling the condition $R_{ij} \leqslant R_c = L/2$. By means of equations (2) and (3) the quantities $\boldsymbol{\mu}_i(t)$ and $\mathbf{M}(t)$ were calculated from the pairwise induced moments $\boldsymbol{\mu}_{ij}(t)$. It was checked that with the used number of molecules and the cutoff radius of $L/2$ the contribution of more distant molecules to $\boldsymbol{\mu}_i(t)$ is negligibly small. This mainly results from the comparison of experimental and simulated values of the effective dipole moment $\bar{\mu}_{\text{eff}}$. The simulated N-molecule CFs have been obtained in intervals of 0·025 ps over a total time interval of 80 ps for a large number of time-origins equally spaced (0·025 ps) in this time interval and extend-

Table 1. Comparison of the technical features of the existing simulations of liquid nitrogen with those of the present study. VS and QPC are the Verlet–Singer and the Quaternion predictor corrector algorithms respectively. L is the box length.

Reference	Temp./ K	Density/ $Å^{-3}$	Number of molecules	Potential model	Algorithm	Time integration step/ps	Total time of simulations/ ps	Cutoff radius	Polarizability model	Number configurations between sampling
[3]	70	0·01866	500	Atom–atom LJ(12-6) [10(a)]	[10(a)]	0·005	110	—	Isotrop.	—
[12]	75·7	0·0175	256	Atom–atom LJ(12-6) + quadrupoles	QPC	0·00324	56	$R_c = L/2$	Isotrop. and anis.	25
	62·8	0·01847								
This study	65	0·01864	256	Atom–atom LJ(12-6) [10(a), (b)]	VS + QPC	0·005	90	$R_c = L/2$	Isotrop. and anis.	5

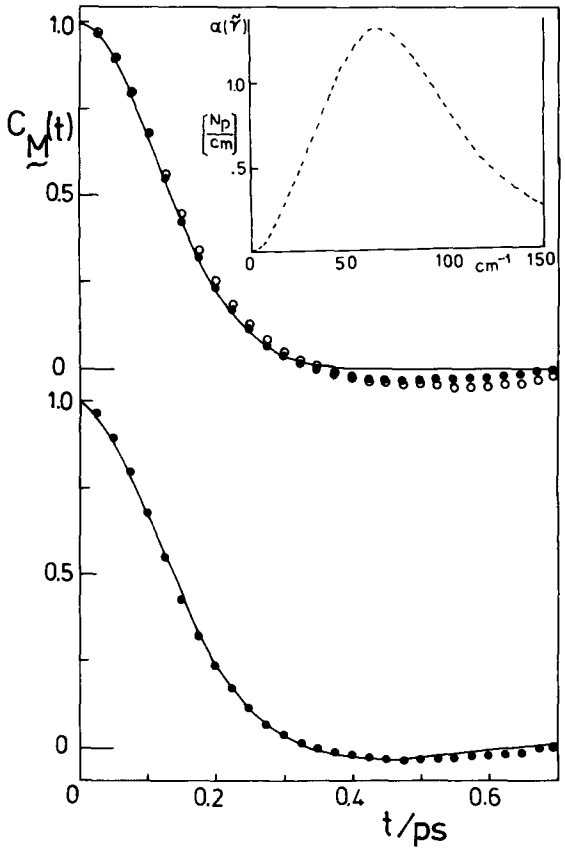

Figure 1. Dipole CFs of liquid nitrogen. ○, simulation with the isotropic model; ●, simulation with the anisotropic model. The solid line represents the CF obtained from the Fourier transform of the experimental spectrum. The insert shows the experimental spectrum [3]. The solid line in the lower CF is obtained by the fit of the Mori function (equation (10)) to the points of the simulation with the anisotropic model.

ing over all 256 molecules. This procedure led to an acceptable statistical error which was, however, larger in the case of the total and cross-CFs than of the self-CFs.

4. Comparison of the simulation with experimental data

Figure 1 gives in the insert an experimental spectrum of liquid nitrogen at 66 K as published in the literature [3]. The total dipole-CF in this figure was calculated by fitting the published spectrum with equation (12) and using the analytical relations between the constants defined in equations (11 *a–h*) and those appearing in (12) to calculate the right-hand side of (11). In order to compare the experimental result to the simulation it is useful to compare in the first instance the corresponding values of the effective dipole moment, defined in (13), as illustrated in table 2. Column 1 of this table gives the experimental value of $\bar{\mu}_{\text{eff}}$, whereas the theoretical values obtained in the present simulation is given in

Table 2. Comparison of experimental (column 1), simulated (columns 3 and 4) and theoretical (column 5) values of the effective dipole moment $\tilde{\mu}_{eff}/10^{-31}$ cm. The theoretical values [8] have been obtained with the same polarizability and quadrupole moment as those used in this simulation.

		Calculated effective dipole moments		
		This simulation		
Experimental	Quadrupole moment used	Isotropic polarizability model	Anisotropic polarizability model	Theory [8]
0·759	−4·760 [20(a)]	0·686	0·737	0·806
	−5·070 [20(b)]	0·720	0·772	0·858

columns 3 and 4. Due to the uncertainty in the experimental value of the molecular quadrupole moment of nitrogen, displayed in column 2, the simulated values of the effective moments are frought with an uncertainty leading to the two different sets of values in the two rows of the table. The difference between the models with an isotropic and an anisotropic polarizability of the nitrogen molecule is of the same order. This result shows that, as far as $\tilde{\mu}_{eff}$ is concerned, the simulation reflects the experiment rather well, provided the adequate value of the quadrupole moment is chosen. Unfortunately, this comparison could not be made with the results of the previous simulation because the relevant data have not been included in the paper. On the basis of the CF however, as given in figure 1, the difference between the experimental and the simulated absorption cannot be so large as the spectra reported by the authors seem to imply.

The simulation data of this study are displayed in figure 1 as empty and black dots for the isotropic and anisotropic model respectively. As can be seen, the agreement between these and the CF derived from the experiment is very good at

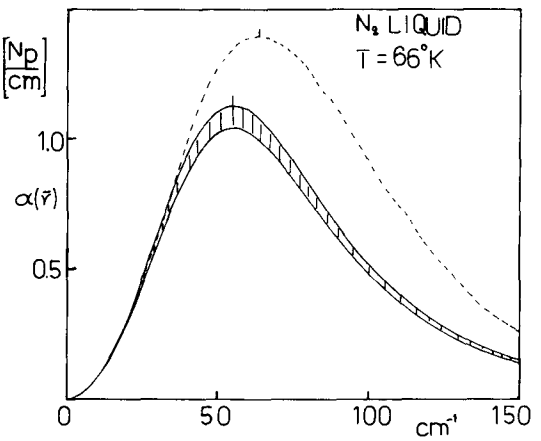

Figure 2. Experimental and simulated spectra of liquid nitrogen (anisotropic model). The broken line represents the experimental spectrum. The shaded range illustrates the range in which the simulated spectrum lies, considering the uncertainty in the experimental value of the quadrupole moment. The simulated spectrum was obtained by the Mori fit equation (10).

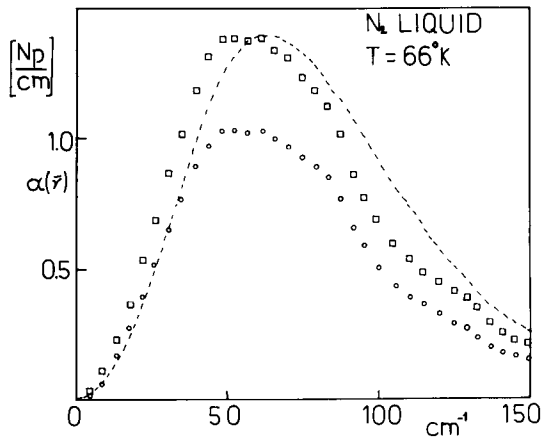

Figure 3. Experimental and simulated spectra of liquid nitrogen. The broken line represents the experimental spectrum. ○, simulation with the anisotropic model and direct Fourier transform by equation (4). □, the same simulated spectrum normalized to the intensity of the experimental spectrum.

short times, i.e. below 0·35 ps. The difference between the isotropic and the anisotropic model does not manifest itself to a significant degree in the correlation functions. Figure 2 illustrates the relation between the experimental spectrum and those obtained by the present simulation with the use of the two values of the quadrupole moment, the shaded area showing the uncertainty due to the incomplete knowledge of the quadrupole moment. It is obvious that the present calculation gives intensities which are nearer to the experimental result than the older simulation does. In order to be able to discuss the shape of the spectra, the simulated spectrum has been normalized to the same intensity as the experimental. The comparison of the two spectra in figure 3 shows, that the positions of the maxima are shifted by approximately $4\,cm^{-1}$. This shift was not observed in the older simulation which, however, was carried out at a temperature between 66 and 76 K instead of 66 K as in our case. In view of the strong shift of the spectrum to higher frequencies with increasing temperature, the observed difference may be attributed to the difference in temperature between the two sets of data.

5. Interpretation of the correlation functions

The CFs derived from the experimentally observed spectra result from the loss of coherence of the total induced dipole moment $\mathbf{M}(t)$ in the sample introduced into the light beam. The corresponding CF $C_{\mathbf{M}}(t)$, as demonstrated by equation (5), is the sum of the self-CF $C_s(t)$ of the molecules and the cross-CF $C_+(t)$ representing the loss of coherence of the dipoles induced in different molecules. Often the total CF has been identified with the self-CF, the neglect of the cross-CF being justified by intuitive arguments. On the other hand, it has been established that at liquid densities the cancellation of the induced dipoles on different molecules is very strong thus the question as to the time dependence of this cancellation effect. The present simulation lends itself to the study of this problem.

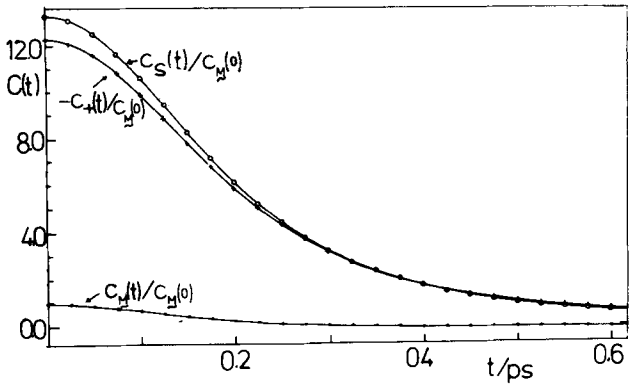

Figure 4. Comparison of the total, self-, and cross-CF of liquid nitrogen. The CFs have been normalized with respect to the total dipole CF.

Figure 4 shows the self-CF the total CF and the negative cross-CF, all three normalized with respect to the total CF. The sign of the cross-CF was changed in order to represent it together with the two others on the positive side of the ordinate axis. The figure illustrates very clearly the amount of cancellation which results in a much lower amplitude of $C_M(t)$ as compared to $C_s(t)$. The difference in the time dependence of the self- and the cross-CF is very small, the correlation time of the self term being smaller by approximately 10 per cent than the cross term. This suggests that the motion of proximate molecules in liquid nitrogen remains coherent over the time interval of some tenths of a picosecond. This result presumably depends upon the nature of the molecules, their anisotropy being an important factor. This also means that the induction process in a dense phase generally involves the production of more than one dipole which partially cancel each other, and it seems that the molecular motion affects this set of dipoles in a coherent way.

The self term of the molecular motion can be further analysed by separating the induced dipole CF into the dipole-modulus CF and the dipole–unit-vector CF. These two CFs are defined by the following equations:

$$C_{s,|\boldsymbol{\mu}|}(t) = \langle |\boldsymbol{\mu}_i(0)| \cdot |\boldsymbol{\mu}_i(t)| \rangle, \tag{14a}$$

$$C_{s,\boldsymbol{\mu}_0}(t) = \langle \boldsymbol{\mu}_{0i}(t) \cdot \boldsymbol{\mu}_{0i}(t) \rangle. \tag{14b}$$

Assuming that the rotation of the induced dipole vector is statistically independent from the change of its modulus the product of $C_{s,|\boldsymbol{\mu}|}(t)$ and $C_{s,\boldsymbol{\mu}_0}(t)$ gives the self-CF

$$C_s(t) \cong C_{s,|\boldsymbol{\mu}|}(t) \cdot C_{s,\boldsymbol{\mu}_0}(t). \tag{15}$$

The results of the simulation of these CFs is illustrated in figure 5. The product-CF, indicated by the dots does not, in contrast to equation (15), coincide with the self-CF. This is an indication that the unit dipole vector and the modulus of the dipole vector are performing motions which are correlated to some extent. This could e.g. mean that if the angle between the dipole vector at $t = 0$ and at $t = t_1$ increases its modulus is, on the average, increasing too. Since this is the case for the isotropic polarizability model also this correlation is an effect of the cage field

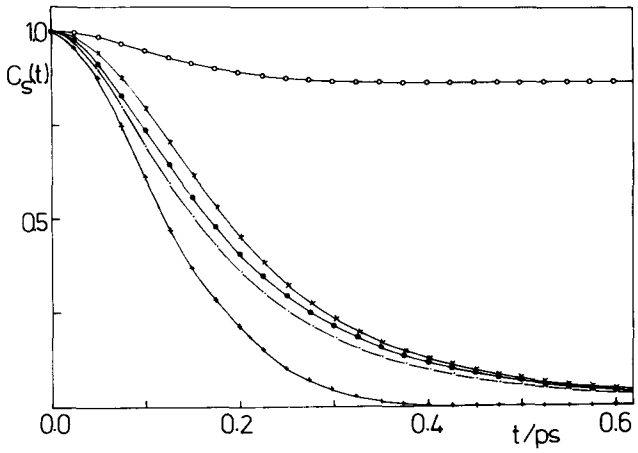

Figure 5. Separation of the self dipole-CF into the CF of the modulus and the unit vector of the induced molecular dipole moment. ○, CF of the modulus of $\boldsymbol{\mu}$; ●, CF of the unit vector of $\boldsymbol{\mu}$; +, the modulus-CF normalized to equal amplitude with the unit vector CF; ×, self dipole-CF; . , CF of the product $C_{s,|\boldsymbol{\mu}|}(t)\,.\,C_{s,\boldsymbol{\mu}_0}(t)$.

motion with respect to the reference molecule. Another salient feature of this figure is the small amplitude of $C_{s,|\boldsymbol{\mu}|}(t)$ which decays to a non-zero long-time value of approximately 0·8. By normalizing both $C_{s,|\boldsymbol{\mu}|}(t)$ and $S_{s,\boldsymbol{\mu}_0}(t)$ to equal amplitudes, as illustrated in figure 5, we see that the correlation time of the modulus is clearly shorter than that of the unit vector. At times longer than 0·2 ps the motion of the induced dipole can be described by a rotating vector displaying only small fluctuations of its modulus. This motion reflects the fluctuation kinetics of the inducing cage field as well as the centre-of-mass motion of the reference molecule. Obviously, the cage field has a long-lived average component which in this time range is not destroyed by the cage motions. Additionally, the motion of the reference molecule within the cage which contributes to the CF, does not bring it into regions with very different values of the cage field. From this we can visualize the inducing cage as producing in the space accessible to the reference molecule a relatively homogeneous electrical field which fluctuates somewhat in magnitude and much more in its direction. We should, however, bear in mind that the model underlying the simulation of the inducing field, i.e. the assumption of a quadrupole field in a homogeneous medium described by a space and time averaged constant dielectric permittivity, oversimplifies the real situation. Actually, the random distribution of polarizable electron density distorts the inducing field to a significant degree.

In order to specify in more detail the relation between the observed self term of the CF function and the single-molecule reorientation we calculated the CF of P_1, the first order Legendre polynomial, $C_1(t)$. Figure 6 shows this $C_1(t)$, the self-term of the induced CF $C_{s,\boldsymbol{\mu}_0}(t)$ and the CF of $\cos\theta$, θ being the angle between the unit vector along the molecular axis and the induced dipole $\boldsymbol{\mu}_{0i}(t)$

$$C_{\cos\theta}(t) = \langle[\boldsymbol{\mu}_{0i}(0)\,.\,\mathbf{u}_i(0)]\,.\,[\boldsymbol{\mu}_{0i}(t)\,.\,\mathbf{u}_i(t)]\rangle. \tag{16}$$

As expected, $C_{s,\boldsymbol{\mu}_0}(t)$ decays at a faster rate than $C_1(t)$ since it is shaped by motions of the reference molecule as well as by translational and rotational

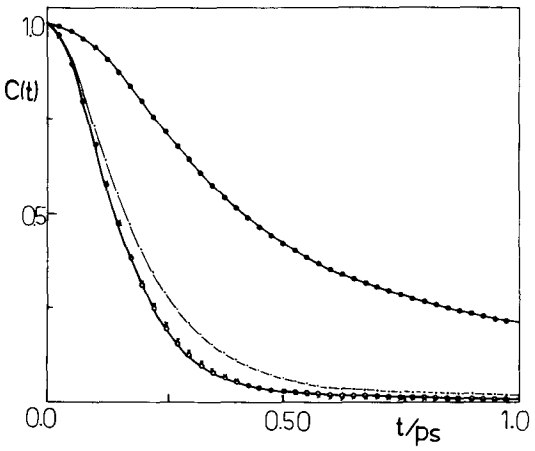

Figure 6. ○, CF of cos θ, θ is the angle between the induced dipole moment and the molecular axis; ●, P_1 Legendre polynomial CF: C_1; . , CF of the unit vector of $\boldsymbol{\mu}$; ×, CF of the product $C_1(t)$. $C_{s,\boldsymbol{\mu}_0}(t)$.

motions of the cage molecules. Furthermore, the rotation of the molecule enters the self-CF as a second-order tensor rotation which is faster than the vector reorientation. On the other hand, $C_{\cos\theta}(t)$ describes the loss of coherence of the angle between the two vectors $\mathbf{u}(t)$ and $\boldsymbol{\mu}_0(t)$ relaxing with $C_1(t)$ and $C_{s,\boldsymbol{\mu}_0}(t)$ respectively. As can be seen in figure 6 the product of these two CFs coincides over the whole time-range studied with $C_{\cos\theta}(t)$ in agreement with the following equation:

$$C_{\cos\theta}(t)/C_{\cos\theta}(0) = C_1(t)C_{s,\boldsymbol{\mu}_0}(t). \tag{17}$$

The validity of such an equation is not a priori obvious but it appears that in the case of liquid nitrogen under the conditions of this simulation any cross correlations between $\mathbf{u}(t)$ and $\boldsymbol{\mu}_{0i}(t)$ can be neglected. The physical implication of this is that the dipole vector CF in liquid nitrogen is predominantly shaped by cage rearrangements and/or translational motions of the reference molecule and to a much lesser degree by single-molecule reorientation. It is important to keep in mind that only $C_1(t)$ and $C_2(t)$ are genuinely single-molecule reorientation CFs, all other CFs reflecting also the translational dynamics of the reference molecule and the many-particle dynamics of the cage rearrangement.

6. Conclusions

An important issue in molecular dynamics of liquids is the question whether different motions of a molecule, like rotation and translation, are sufficiently independent to be separable in a physically meaningful way, and to what extent this can be realized by computer simulation. Specifically, we must discuss the question as to the contribution of translational and rotational motions to be interaction induced experimental spectra.

Some of the observations reported for the model-liquid nitrogen in this study are summarized below because they can be helpful in discussing this issue.

(*a*) The large cancellation of molecular dipoles in liquid nitrogen (figure 4) by more than 90 per cent points to a relatively symmetric arrangement of the mole-

cules. This cancellation, which is reflected in the cross-CF, decays at a rate similar to the self-CF. As a consequence, the total induced dipole CF in this liquid is shaped by both, the self- and the cross-term in a very critical way. Actually, its correlation time is by 20 per cent smaller than the correlation time of the self-term. Note that both the self-term and the cross-term are collective properties containing, in principle, rotational as well as translational contributions.

(*b*) The small effect on the correlation times of the self- and the cross-term obtained by introducing an anisotropic molecular polarizability model (figure 1) indicates that the rotation of the reference molecule does not greatly contribute to the decay of the correlation functions.

(*c*) The long-time limit of 0·86 of the induced dipole modulus-CF (figure 5) indicates that most of the decay of the dipole-CF at times above 0·2 ps occurs by rotation of the induced dipole as a consequence of cage rearrangements. For this we have to consider rotations as well as translations of the cage molecules.

(*d*) The correlation time of the self-term (figure 5) is smaller than the correlation times of either the P_1 or the P_2 Legendre polynomials. This also indicates that the rotation of the reference molecule is not important in determining the self-CF. The conclusion that not the rotation of the reference molecule, but mainly the cage rearrangement as well as the translation of the reference molecule cause the decay of the self-CF is also corroborated by the relatively small effect of $C_1(t)$ on the self-term to produce the CF of the angle between the molecular axis and the induced dipole vector.

(*e*) The present simulation reproduces the experimental far infrared spectra in shape, position and amplitude to such a degree (figure 2) that it seems reasonable to infer from the properties of the simulation model to the real liquid.

The authors gratefully acknowledge the financial support of the 'Deutsche Forchungsgemeinschaft', the 'Fonds der Chemischen Industrie', the 'Zentrum für interdisziplinäre Forschung der Universität Bielefeld' and the helpful contribution provided by the fund 'Alexander Jost'.

References

[1] Bosomworth, D. R., and Gush, H. P., 1965, *Can. J. Phys.*, **43**, 751.
[2] (a) Gebbie, H. A., Stone, N. W. B., and Williams, D., 1963, *Molec. Phys.*, **6**, 215. (b) Heastie, R., and Martin, D. H., 1962, *Can. J. Phys.*, **40**, 122.
[3] Buontempo, U., Cunsolo, S., Jacucci, G., and Weis, J. J., 1975, *J. chem. Phys.*, **63**, 2570.
[4] Jones, M. C., 1970, *Natn. Bur Stand., Tech. Note* 390.
[5] Buontempo, U., Cunsolo, S., and Jacucci, G., 1971, *Molec. Phys.*, **21**, 381.
[6] (a) Poll, J. D., 1978, *Intermolecular Spectroscopy and Dynamical Properties of Dense Systems*, edited by J. van Kranendonk (North-Holland). (b) Ladd, A. J. C., Litovitz, T. A., and Montrose, C. J., 1979, *J. chem. Phys.*, **71**, 4242. (c) Madden, P. A., and Tildesley, D. J., 1983, *Molec Phys.*, **49**, 193.
[7] (a) Birnbaum, G., in [6 (a)]. Birnbaum, G., and Sutter, H., 1981, *Molec. Phys.*, **42**, 21. (b) Murthy, C. S., and Singer, K., 1982, *Chem. Phys. Lett.*, **90**, 95.
[8] Steele, W. A., and Birnbaum, G., 1980, *J. chem. Phys.*, **72**, 2250.
[9] Guillot, B., and Birnbaum, G., 1983, *J. chem. Phys.*, **79**, 686.
[10] (a) Barojas, J., Levesque, D., and Quentrec, B., 1973, *Phys. Rev.* A, **7**, 1092. (b) Quentrec, B., and Brot, C., 1975, *Phys. Rev.* A, **12**, 272. (c) Cheung, P. S. Y., and Powles, J. G., 1975, *Molec. Phys.*, **30**, 921. (d) Cheung, P. S. Y., and Powles, J. G., 1976, *Molec. Phys.*, **32**, 1383.

[11] BROT, C., 1975, *Dielectric and Related Molecular Processes*, Vol. 2, edited by M. Davies (Specialist Periodical Reports) (The Chemical Society London), p. 1.
[12] STEELE, W. A. (private communication).
[13] BUCKINGHAM, A. D., 1959, *Q. Rev. chem. Soc.*, **93,** 183.
[14] APPLEQUIST, J., CARLAND, J. R., and FUNG, K. K., 1972, *J. Am. chem. Soc.*, **94**, 2952.
[15] DORFMÜLLER, TH., and SAMIOS, J., 1984, *Molec. Phys.*, **53,** 1167.
[16] (a) DAVIES, G. J., and EVANS, M., 1976, *J. chem. Soc., Faraday II*, **72,** 1194. (b) EVANS, M., and DAVIES, G. J., 1976, *Adv. mol. relax. Processes*, **9,** 129.
[17] (a) VERLET, L., 1976, *Phys. Rev.*, **98,** 159. (b) SINGER, K., TAYLOR, A., and SINGER, J. V. L., *Molec. Phys.*, **33,** 1757.
[18] (a) EVANS, D. J., 1977, *Molec. Phys.*, **34,** 317; EVANS, D. J., and MURAD, S., 1977, *Molec. Phys.*, **34,** 327. (b) FINCHAM, D., *Information Quarterly-CCP5*, No. 2, September 1981, p. 6.
[19] (a) ZWANZIG, R., and AILAWADI, N. K., 1969, *Phys. Rev.*, **182,** 280. (b) FRENKEL, D., in [6 (a)].
[20] (a) BUCKINGHAM, A. D., DISCH, R. L., and DUMMUR, D. A., 1968, *J. Am. chem. Soc.*, **90,** 3104. (b) STOGRYN, D. E., and STOGRYN, A. P., 1966, *Molec. Phys.*, **11,** 371.